Author's personal copy

Biomaterials 34 (2013) 5926–5936

Contents lists available at SciVerse ScienceDirect

Biomaterials

journal homepage: www.elsevier.com/locate/biomaterials

Enhanced reconstruction of long bone architecture by a growth factor mutant combining positive features of GDF-5 and BMP-2

Kerstin Kleinschmidt [a,1], Frank Ploeger [b], Joachim Nickel [c], Julia Glockenmeier [a], Pierre Kunz [a], Wiltrud Richter [a,*]

[a] Research Centre for Experimental Orthopaedics, Orthopaedic University Hospital Heidelberg, Schlierbacher Landstrasse 200a, 69118 Heidelberg, Germany
[b] Biopharm GmbH, Headquarter Heidelberg, Czernyring 22, 69115 Heidelberg, Germany
[c] University Clinic Wuerzburg, Chair of Tissue Engineering and Regenerative Medicine, Schneider-Strasse 2, 97080 Wuerzburg, Germany

ARTICLE INFO

Article history:
Received 21 February 2013
Accepted 16 April 2013
Available online 13 May 2013

Keywords:
Osteogenesis
Angiogenesis
Bone mineral density
Growth factor
Bone morphogenetic protein
In vivo micro-CT

ABSTRACT

Non healing bone defects remain a worldwide health problem and still only few osteoinductive growth factors are available for clinical use in bone regeneration. By introducing BMP-2 residues into growth and differentiation factor (GDF)-5 we recently produced a mutant GDF-5 protein BB-1 which enhanced heterotopic bone formation in mice. Designed to combine positive features of GDF-5 and BMP-2, we suspected that this new growth factor variant may improve long bone healing compared to the parent molecules and intended to unravel functional mechanisms behind its action. BB-1 acquired an increased binding affinity to the BMP-IA receptor, mediated enhanced osteogenic induction of human mesenchymal stem cells versus GDF-5 and higher VEGF secretion than BMP-2 *in vitro*. Rabbit radius defects treated with a BB-1-coated collagen carrier healed earlier and with increased bone volume compared to BMP-2 and GDF-5 according to *in vivo* micro-CT follow-up. While BMP-2 callus often remained spongy, BB-1 supported earlier corticalis and marrow cavity formation, showing no pseudojoint persistence like with GDF-5. Thus, by combining positive angiogenic and osteogenic features of GDF-5 and BMP-2, only BB-1 restored a natural bone architecture within 12 weeks, rendering this promising growth factor variant especially promising for long bone regeneration.

© 2013 Elsevier Ltd. All rights reserved.

1. Introduction

Callus induction, sufficient blood supply and remodeling of a new bone matrix are prerequisites for well-organized bone formation after fracture and in large bone defects after trauma or tumor resection [1,2]. Metabolic degradation of the extracellular matrix (ECM) is both precondition and consequence of blood vessel invasion indicating narrow relationships between ECM formation, degradation and angiogenesis [3]. Though, the interplay of osteogenesis and angiogenesis in bone regeneration is still poorly defined, as are the prerequisites to restore a natural corticalis and trabecular structure of long bones [4,5].

The local use of bone morphogenetic protein (BMPs) family members as bone inducers in not healing defects is a strategy that has already been pursued for over a decade [6–8]. Although gene expression of several BMP family members was significantly lower in non-unions compared to standard healing fractures [9], still only a few growth factors including BMP-2, BMP-7, and GDF-5 are available for clinical use in bone regeneration [10].

While the osteoinductive effect of BMP-2 is not only well investigated *in vitro* [11], but is also documented in several animal studies [12,13], little is known about its exact contribution to osteoinduction versus angiogenesis in the healing callus. GDF-5, a key stabilizer of cartilage during embryogenic development [14] has received special attention as its functional loss caused delayed bone fracture healing [15] while local application was able to enhance bone regeneration [16–18]. Overall, the therapeutic potential for bone healing of GDF-5 is less well studied than that of BMP-2 and even fewer studies directly compared the effectiveness of both proteins [8,19,20]. Since GDF-5 was postulated to be less osteoinductive than BMP-2 [19], and suspected to be one of the molecules inducing angiogenesis in the physiological bone

* Corresponding author. Tel.: +49 (0) 6221 969254; fax: +49 (0) 6221 969288.
E-mail addresses: kerstin.kleinschmidt@merckgroup.com (K. Kleinschmidt), fploeger@biopharm.de (F. Ploeger), joachim.nickel@uni-wuerzburg.de (J. Nickel), julia.glockenmeier@med.uni-heidelberg.de (J. Glockenmeier), pierre.kunz@med.uni-heidelberg.de (P. Kunz), wiltrud.richter@med.uni-heidelberg.de (W. Richter).
[1] Current address: Merck KGaA, Biologics and Immunology – Osteoarthritis, Frankfurter Straße 250, 64293 Darmstadt, Germany.

0142-9612/$ – see front matter © 2013 Elsevier Ltd. All rights reserved.
http://dx.doi.org/10.1016/j.biomaterials.2013.04.029

Author's personal copy

formation process of vertebrates [21], we speculated that combining the higher osteogenicity of BMP-2 with the suspected superior angiogenic features of GDF-5 in a new growth factor molecule could lead to superior bone regeneration. Our recent work demonstrated, that by swapping selected amino acids in the proposed BMP receptor binding region of GDF-5 to residues present in BMP-2, the newly created protein variant (GDF-5M453V/M456V here called BB-1) acquired an enhanced heterotopic bone formation capacity than GDF-5 in mice [22].

In this study we now asked whether this new growth factor variant may improve long bone healing compared to the two parent molecules GDF-5 and BMP-2. To unravel functional mechanisms behind its action we assessed the BMPR-I and BMPR-II affinity of BB-1 and GDF-5, and dissected the functional *in vitro* activity on cultured human mesenchymal stem cells (MSC) which are clinically relevant osteoprogenitor cells. Beyond quantitation of osteogenesis via upregulation of alkaline phosphatase (ALP) enzyme activity, we quantified secretion of the two angiogenic molecules vascular endothelial growth factor (VEGF) and angiopoietin 1 (ANGPT1) after treatment of cultures with BMP-2, GDF-5, and BB-1. Furthermore, the metabolism of human umbilical vein endothelial cells (HUVEC) in response to the growth factors was assessed. The functionality of recombinant BB-1 protein to reconstruct hollow bone was studied in comparison to equal doses of BMP-2 and GDF-5 after local treatment of long bone critical size defects in the rabbit radius. Bone healing could be followed over time within the same animals using a custom-adapted *in vivo* micro-CT scanner for 12 weeks.

2. Materials and methods

2.1. Growth factors

Recombinant human growth and differentiation factor-5 (GDF-5; Biopharm GmbH, Heidelberg, Germany) and recombinant human bone morphogenetic protein-2 (BMP-2) (R&D Systems, Minneapolis, USA) were stored at −80 °C until use. A variety of swap mutants introducing BMP-2 derived residues into the putative BMPR-I binding region of GDF-5 were created as described previously [22]. The proteins were dissolved in 10 mM HCl.

2.2. SPR Biacore measurements

A Biacore2000 system (Biacore, GE Healthcare, Chalfont St. Giles, GB) was used for all biosensor experiments. Measurements were carried out as described in detail [23]. In brief, approximately 250 resonance units (RU) of N-biotinylated receptor ectodomains of BMPR-IA, BMPR-IB, or BMPR-II were immobilized to streptavidin coated CM5 biosensor chips. Interaction sensorgrams were recorded at a flow rate of 10 μl/min. The experiments were carried out in duplicate using ligand concentrations of 10, 20, 30, 40, 60 and 80 nM. All apparent binding affinities were obtained using BIAevaluation v. 2.2.4 (Biacore, GE Healthcare, Chalfont St. Giles, GB). The affinities for ligand type I receptor interaction were derived by fitting the kinetic data to a 1:1 Langmuir binding model (K_D (kin)). Due to too fast binding kinetics (exceeding 10^6 M^{-1} s^{-1} (for k_{on}) and 10^{-2} s^{-1} (for k_{off})) the apparent binding affinities for the ligand:BMPR-II interaction were determined from the dose dependency of equilibrium binding (K_D (eq)).

2.3. Growth factor induced ALP activity in C2C12 cells

C2C12 cells were plated in alpha-MEM (Sigma, Taufkirchen, Germany), supplemented with 2 mM L-glutamine (Invitrogen) and 10% fetal calf serum (FCS, Invitrogen). After 24 h, cells were stimulated with a 1:3 dilution series of 1200 ng/ml of GDF-5, BMP-2, and BB-1 respectively in triplicate measurements. After 72 h cells were washed with PBS and extracted with 1% Nonidet-40, 0.1 M glycine pH 9.6, 1 mM $MgCl_2$ and 1 mM $ZnCl_2$ for 15–18 h at 37 °C. Conversion of 10 mM p-nitrophenylphosphate as a substrate in 0.1 M glycine pH 9.6, 1 mM $MgCl_2$ and 1 mM $ZnCl_2$ was measured as OD (Tecan Spectra Rainbow, TECAN, Crailsheim, Germany) at 405 nM under consideration of lysis buffer blank value subtraction.

2.4. MSC isolation and cultivation

Human bone marrow aspirates were obtained from 6 donors (42–74 years, mean: 63 ± 11.67 years) undergoing total hip replacement. All procedures were approved by the institutional ethics committee and informed consent was obtained from all donors. MSC were isolated as described previously [24,25]. Briefly, cells were fractionated using Paque™Plus (Amersham Biosciences, Uppsala, Sweden) and seeded in high-glucose Dulbecco's modified Eagle's medium (DMEM, Invitrogen), 2% FCS, 100 IU/ml penicillin and 100 μl/ml streptomycin (both Seromed/Biochrom KG, Berlin, Germany), 40% MCDB201, 0.02 μM dexamethasone, 0.1 mM ascorbic acid-2-phosphate, 2% ITS supplement, 10 ng/ml rhPDGF BB (Sigma), and 10 ng/ml rhEGF (Strathmann Biotech, Hamburg, Germany) until the third passage.

2.5. Osteogenic induction of MSC

MSC were subjected to osteogenic induction as described earlier [26]. Briefly, 35,000 MSC were either plated in osteogenic medium (om); DMEM high glucose, 10% FCS, 0.1 μM dexamethasone, 0.17 mM ascorbic acid-2-phosphate, 10 mM β-glycerol phosphate, 100 IU/ml penicillin and 100 μl/ml streptomycin, or in a basal medium (bm); DMEM, 10% FCS, 100 IU/ml penicillin and 100 μl/ml streptomycin, respectively. Either 50 or 500 ng/ml GDF-5, BB-1, BMP-2 or no growth factor was added, for 21 days respectively. Then monolayers were stained with alizarin red (Waldeck GmbH&Co. KG, Muenster, Germany) which was afterwards quantified using cetylpyridinium chloride [27]. ALP was quantified at day 21 after lysis with 500 μl 1% Triton-X100. Fifty μl lysate were diluted in 50 μl ALP-buffer and conversion of 10 mg/ml p-nitrophenylphosphate (Sigma–Aldrich) in 0.1 M glycine, 1 mM $MgCl_2$, 1 mM $ZnCl_2$ (pH 9.6) was measured in an ELISA reader at 405 nm. Data were normalized to the total protein content as determined with the Pierce Micro BCA Protein Assay Reagent Kit (Thermo Scientific, Rockford IL, USA).

2.6. Analysis of angiogenic parameters in MSC

DuoSet ELISA Development System for human VEGF and Quantikine Angiopoietin1 Immunoassay (both R&D Systems) were used as described by the manufacturer. Medium that was not exposed to cells, but contained 50 or 500 ng/ml GDF-5, BB-1, BMP-2 or no growth factor respectively was measured as group specific blank. For gene expression analysis total RNA was extracted from cultured cells at day 21 using a standard guanidine thiocyanate/phenol-chloroform extraction technique (peqGOLD TriFast, PeqLab, Erlangen, Germany). Polyadenylated messenger RNA (mRNA) was isolated using oligo (dT) coupled to magnetic beads (Dynabeads, Invitrogen), according to the manufacturer's instructions. Messenger RNA was eluted in 12 μl 10 mM TrisHCl and 20 ng were subjected to cDNA synthesis by using OmniScript reverse transcriptase (Invitrogen) in the presence of dNTPs (PeqLab), oligo (dT)12–18 Primer (Invitrogen), RNase OUT (Invitrogen) and DTT, according to the manufacturer's instructions. Quantitative real-time PCR was performed in a LightCycler instrument (Roche Diagnostics). 2 μl of 1:5 diluted cDNA were amplified using human gene specific primers listed in Table 3 (MWG Biotech). HUVEC, human lung tissue, SaOs-cells or human osteoblasts respectively were analyzed in parallel as positive controls. Water served as a negative control. The conditions of the PCR reaction were 94 °C for 10 min and 40 cycles consisting of 94 °C for 5 s, 60 °C (ALP) or 58 °C (all other genes) for 7 s, 72 °C for 8 s (β-actin, ANGPT2, VEGF), 14 s (ANGPT1) or 20 s (ALP) respectively.

2.7. Effect on metabolism of endothelial cells

Fresh endothelial cells (HUVEC) were isolated from human umbilical veins using a protocol described elsewhere [28]. Briefly, PBS rinsed cells were centrifuged at 300 g for 10 min and plated on gelatine (0.4%) coated culture flasks (25 cm^2) in EBM-2 (Lonza Ltd, Basel, Switzerland) with 100 IU/ml penicillin, 100 μl/ml streptomycin and 25 mM N-2-Hydroxyethylpiperazine-N-2-ethane sulphonic acid (HEPES, Sigma). WST (water soluble tetrazolium)-1 based proliferation assay was performed after 4 passages in 96-well plates with HUVEC of 3 donors in triplicate. 1×10^3, 1.2×10^3, 1.5×10^3, 1.7×10^3 and 2×10^3 cells/well were seeded to determine optimal cell number individually for each donor after 24 h. 5, 20 or 500 ng/ml of GDF-5, BB-1, BMP-2 or no growth factor respectively were added. 30 μl reagent WST-1 were added after 24 h of adhesion and OD was measured every 60 min over 5 h at 450 nm in a Microplate Reader.

2.8. Animal experiments

Rabbits were treated in compliance with the guiding principles in the care and use of animals. The Committee on animal experimentation of Baden-Wuerttemberg approved the experiments with the reference numbers AZ35-9185.81/A-3/08 (micro-CT-establishment) and AZ35-9185.81/G73/07 (main study). Collagen sponges of equine origin, (Kollagen-resorb, Resorba GmbH Nuernberg, Germany) were cut into pieces of 2 cm × 0.5 cm and lyophilized with the proteins or buffer. Prior to implantation sponges were soaked with sterile saline. Thirty-eight 6 month old female New Zealand White rabbits were used. In a pilot experiment $n = 2$ rabbits per group were implanted with collagen sponges augmented with 20 μg and $n = 2$ with 50 μg BMP-2, GDF-5 or BB-1 and $n = 4$ rabbits with untreated defects for dose finding and establishment of *in vivo* micro-CT scanning. For the main experiment $n = 5$ additional animals were treated with collagen sponges loaded with saline or 20 μg of either BMP-2, GDF-5 or BB-1. Statistical analysis of μCT findings was made of all animals treated with 20 μg growth factor ($n = 7$ per group). Briefly, a 15-mm segmental defect in the middle of the diaphysis of the radius was created using a

Author's personal copy

handsaw. As the proximal and distal endings of the radius are adnated to the ulna, no additional fixation of the defect gap is needed. The collagen sponge was placed into the gap and the wound was closed in three layers. *In vivo* micro-CT was performed directly postoperatively, and after 4, 8 and 12 weeks. Rabbits were euthanized after 12 weeks and specimens were resected for bone mineral density measurement and histology.

2.9. Micro-CT analysis

To allow *in vivo* scanning of rabbit forelegs, a commercially available device (1076, Skyscan, Antwerp) was modified by designing a bedding solution that was constructed customized by RJL Micro&Analytics (Karlsdorf-Neuthard, Germany). The modification enabled positioning the animal beyond the system while only the foreleg was fixed in an aluminum tube transporting the region of interest horizontally into the course of x-ray beam (Supplementary Fig. S1). In a pilot study feasibility and scanning parameters were determined. Proximate scans were performed using a 0.5 mm aluminum filter with the following settings: 48 kV, 200 μA, 320 ms, spatial resolution = 17.7 μm^3/voxel and rotation step = 0.6°. Parameters were analyzed using CTAn® analysis software (Skyscan) with a lower gray level set at 40 and an upper gray level set at 255 to define mineralized callous tissue and depicted following ASBMR nomenclature [29]. 3D-videos were made using CTVox® (Skyscan). "Bridging" (yes/no) was defined as a mineralized structure extending from one defect ending throughout the callus to the other defect ending with new mineralized tissue reaching at least 50% of thickness of the previous radius. To measure this, a line was extrapolated between the ulna-sided corticalis proximal and distal of the defect and tissue thickness above this line was measured at a 90° angle. The volume of interest (VOI) was determined in its proximal and distal dimension by choosing the middle of the defect and taking the same number of 200 slices which is corresponding to 7 mm into each direction (=14 mm total). An interpolated VOI, excluding the ulna, was shrink wrapped exactly to the outer bone boundaries (Fig. 4). For Ma.V analysis the total shrinked volume describing the total callus volume including not radiopaque cavities was measured (BV) and the mineralized volume (Md.V) was subtracted as Ma.V = BV − Md.V.

2.10. Histology

Retrievals from animals treated with 20 μg or 50 μg BMP-2, GDF-5 or BB-1 and from controls were fixed, decalcified in EDTA, paraffin embedded and 5 μm serial longitudinal sections from 20 μg groups and transverse sections of 50 μg groups were cut to the middle of the defect. Alternate sections were stained with trichrome-Masson-Goldner staining (Masson-Goldner Kit 1.00485 Merck), Hematoxylin&Eosin (both Sigma), Safranin-O (SafraninT84120 Fluka, FastGreen1A304 Chroma), anti-CD31 (cloneJC70A, DAKO), anti-collagen-type-I (cloneI-8H5, MP Biomedicals) or anti-collagen-type-II (cloneII-4C11, MP Biomedicals) following standard protocols. Aligned overview microphotographs (Axioplan2, AxiovisionRelease4.6.3, Zeiss) of total slices were made to allocate adequacy of micro-CT based analysis. Magnifications were photographed at the proximal (prox) and distal (dist) defect endings and in the middle (mid) of defects.

2.11. Bone mineral density

Bone mineral density (BMD) defined as the volumetric density of calcium hydroxyapatite in g/cm^3 was analyzed as described in the manufacturer's method note (Skyscan). Briefly, BMD was calibrated by means of two customized phantoms with densities of 0.25 g/cm^3 and 0.75 g/cm^3 hydroxyapatite, respectively and diameters comparable to that of rabbit long bone (Ø 8 mm). Reconstruction was performed using houndsfield units with an interval of 0–0.02 HU for all BMD scans. A different interpretation of the density measurement was used for trabecular versus cortical bone as the volumetric density of thin trabecular structures is generally undermeasured due to the partial volume effect. The trabecular BMD measurement was in parts a medullar BMD and was therefore calculated from a VOI excluding cortical bone. Cortical bone was read out from a VOI excluding medullar bone and determined by a less sensible restricted mean value for all groups.

2.12. Statistical analysis

Related samples from *in vitro* experiments were analyzed using non-parametric Wilcoxon signed-rank test as the values were not distributed normally. As *in vivo* data were independent, ordinal, and normally distributed, non-parametric Mann–Whitney-*U* test was used for calculation of differences in medians. For Md.V, BV and Ma.V each time point was calculated separately (adjusted alpha-level and Bonferroni correction). *P*-values of less than 0.05 were regarded as significant in all experiments and tests.

3. Results

3.1. Increased BMPR-IA binding affinity of BB-1 and enhanced ALP activation in C2C12 cells

Exchange of methionines to valines at positions 453 and 456 in the amino acid sequence of GDF-5 resulted in a 10.8-fold increase in the BMPR-IA binding affinity of BB-1 according to Biacore binding analysis. The apparent K_D-values were 21.50 nM ± 38.75% for GDF-5 and 1.99 nM ± 48.65% for BB-1, while BMPR-IB and BMPR-II binding was unaltered (Table 1). If, as intended, the increased affinity of BB-1 mediates a higher BMPR-IA activation, this should become evident on a cell line with predominant expression of BMPR-IA over BMPR-IB like the mouse premyoblastic cell line C2C12 [30]. Strong dose dependent induction of ALP activity was observed with BMP-2 while ALP response was significantly lower after treatment with GDF-5. Remarkably, BB-1 induced significantly elevated ALP activity compared to GDF-5 (Fig. 1A) up to values similar to BMP-2.

3.2. Enhanced osteogenic in vitro differentiation of MSC with BB-1

Standard osteogenic medium conditions (om) induced strong mineral deposition by human MSC cultures within 3 weeks ($p < 0.001$) compared to basal medium (no dexamethasone, no ascorbic acid-2-phosphate, no β-glycerophosphate) according to normalized alizarin red quantification (Fig. 1B). None of the tested growth factor treatments resulted in a significantly higher mineralization on top of the induction with osteogenic medium alone. BB-1 treated MSC (500 ng/ml) showed a significantly higher ALP activity (1.45-fold, $p < 0.02$) than GDF-5 treated cells and controls (Fig. 1C). As the protein content of cell lysates was equal in all groups independent of growth factor dosage, there was no evidence for negative effects of the growth factor formulations on cell metabolism. Taken together this demonstrated that the exchange of two amino acids in GDF-5 enabled the BB-1 protein to induce stronger osteogenic *in vitro* differentiation of human MSC compared to GDF-5.

3.3. Angiogenic marker secretion by MSC and effect of BB-1 on metabolism of endothelial cells

VEGF gene expression levels of MSC were variable between cultures from different donors (Fig. 2A). However, significantly

Table 1
Biacore binding analysis of GDF-5 and BB-1 to BMP-receptors.

Immobilized receptor	Parameter	GDF-5 wt			BB-1		
		Mean	SD	SD (%)	Mean	SD	SD (%)
BMPR-IA	kon (1/M*s)	1.81E+05	3.65E+04	20.13	1.38E+05	3.15E+04	22.82
	koff (1/s)	3.90E-03	7.26E-04	18.62	2.75E-04	7.10E-05	25.83
	KD kin (nm)	21.50		38.75	1.99		48.65
BMPR-IB	kon (1/M*s)	3.64E+05	5.24E+04	14.373559	3.24E+05	4.86E+04	15.00
	koff (1/s)	4.60E-04	1.40E-04	30.434783	3.40E-04	1.14E-04	33.53
	KD kin (nM)	1.26		44.81	1.05		48.53
BMP-RII	KD eq (nM)	39.25	6.36	16.19	42.53	7.43	17.48

Author's personal copy

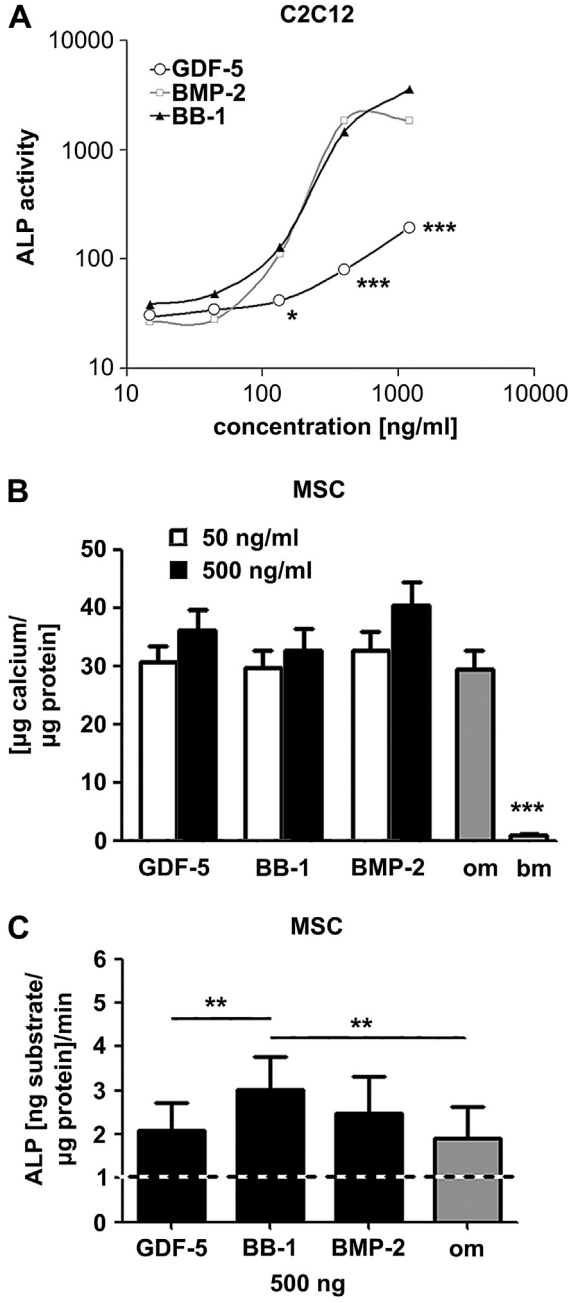

Fig. 1. Effect of growth factors on osteogenic *in vitro* induction. A) C2C12 cells were treated with growth factors for 3 days and ALP activity was measured in lysed cells. Log transformed data are mean ± SD of triplicate measurements ($^{*}p < 0.05$, $^{***}p < 0.01$ vs. all other groups). B) After 21 days of culture alizarin assay was performed on MSC monolayer culture in osteogenic medium (om) with or without growth factors respectively or in basal medium (bm) without dexamethasone, vitamin C and β-glycerophosphate. C) Alkaline phosphatase activity was normalized to total protein content of lysates and related to bm (horizontal dashed line) 50 ng/ml growth factor, was applied. B,C) Data are mean ± SEM of 6 experiments, $^{**}p < 0.02$, $^{***}p < 0.01$ vs. all other groups.

lower VEGF protein levels were observed in culture supernatants from BMP-2 treated cells compared to those from BB-1 ($p < 0.02$) or untreated control cells ($p < 0.05$ Fig. 2B). Gene expression levels of ANGPT1 were significantly lower in BMP-2 treated cells than in controls ($p = 0.05$) and a tendency for lower expression was observed in BMP-2 compared to GDF-5 or BB-1 treated cultures (Fig. 2C). In line, BMP-2 slightly but significantly reduced ANGPT1 protein secretion into culture supernatants compared to all other groups ($p < 0.02$, Fig. 2D). In contrast, BB-1 and wild type GDF-5 did not reduce secretion of VEGF and ANGPT1 by MSC in osteogenic medium. In order to investigate direct effects of the growth factors on human endothelial cells, three different concentrations (5, 20 and 500 ng/ml) were tested on HUVEC of 3 donors in triplicate (Fig. 2E). Since there were no obvious differences between doses, data were analyzed together to compensate for donor variability. The mean mitochondrial cell metabolism of HUVEC from all experiments was reduced within 24 h—79% of control levels by GDF-5 ($p < 0.002$), to 71% of control levels by BMP-2 ($p < 0.002$) and to 84% of control levels by BB-1 (not significant). This suggested some antiproliferative effect for the factors, with BMP-2 effecting a significantly lower mean growth rate than BB-1 ($p < 0.05$).

3.4. BMP-2, GDF-5 and BB-1 enhanced bone defect bridging

Decisive intergroup differences were seen during early healing of critical size (CSD) radius defects in NZW rabbits after single local application of growth factor protein immobilized on an equine native collagen sponge. All BB-1 treated defects (9/9) were bridged 4 weeks post surgery, while only 56% (5/9) of GDF-5 and 33% (3/9) of BMP-2 treated defects were bridged with mineralized tissue as judged by micro CT analysis (Table 2, Fig. 3A, Supplementary Videos 1–4). Eight weeks post surgery all BMP-2 treated (9/9), and 89% of GDF-5 treated (8/9) defects were bridged. None (0/7) of the control defects bridged during the total observation time of 12 weeks nor did the GDF-5 treated defect that was not bridged after 8 weeks.

Supplementary video related to this article can be found at http://dx.doi.org/10.1016/j.biomaterials.2013.04.029.

Micro-CT-scans showed in 78% (7/9) of GDF-5, in 78% (7/9) of BMP-2 and in 11% (1/9) of BB-1 treated defects the formation of a gap disrupting the calcified callus 4 weeks post surgery. In all BMP-2 and BB-1 treated animals this gap had disappeared after 8 weeks, while it manifested in 5/9 of the GDF-5 treated defects even after 12 weeks (Table 2, Fig. 3A, Supplementary Video 3). Histological staining of this region in GDF-5 treated defects presented tissue positive for glycosaminoglycans and collagen-type-II but negative for collagen-type-I with cells showing a chondrogenic phenotype (Fig. 3B–D). The extracellular matrix was not calcified as proven by micro-CT and showed cartilaginous architecture including lacunas fulfilling histological criteria of hyaline-like articular cartilage.

3.5. Accelerated and enhanced neo-bone formation by BB-1

The mineralized callus volume (Md.V) was significantly increased by all tested BMP-family members compared to controls ($p < 0.01$) (Fig. 4). Four weeks post surgery the Md.V was significantly higher in BB-1 treated than in BMP-2 or GDF-5 (1.9-fold, $p < 0.01$) treated animals (Fig. 4B) and was 14-fold higher than in untreated defects ($p < 0.001$). Total callus formation (BV) including non-mineralized cavities of BB-1 treated defects was 13-fold higher than in controls ($p < 0.001$) and 1.9-fold higher than in GDF-5 and BMP-2 groups after four weeks ($p < 0.001$) (Fig. 4C). Still, after 12 weeks, BV in BB-1 treated defects was 1.7-fold higher than in BMP-2 and 1.8-fold higher than in GDF-5 treated defects ($p < 0.01$). GDF-5 and BMP-2 induced callus was equal in size at all time points according to Md.V and BV values providing no evidence for reduced bone healing capacity of GDF-5 versus BMP-2 in our model. Marrow cavity volume (Ma.V) was significantly larger in BB-1 versus controls (Supplementary Video 1) while no intergroup differences were observed between BMP-2, GDF-5 treated defects and controls at all time points (Fig. 4D, $p < 0.001$). Overall, this demonstrated an accelerated and enhanced neo-bone formation by BB-1.

Author's personal copy

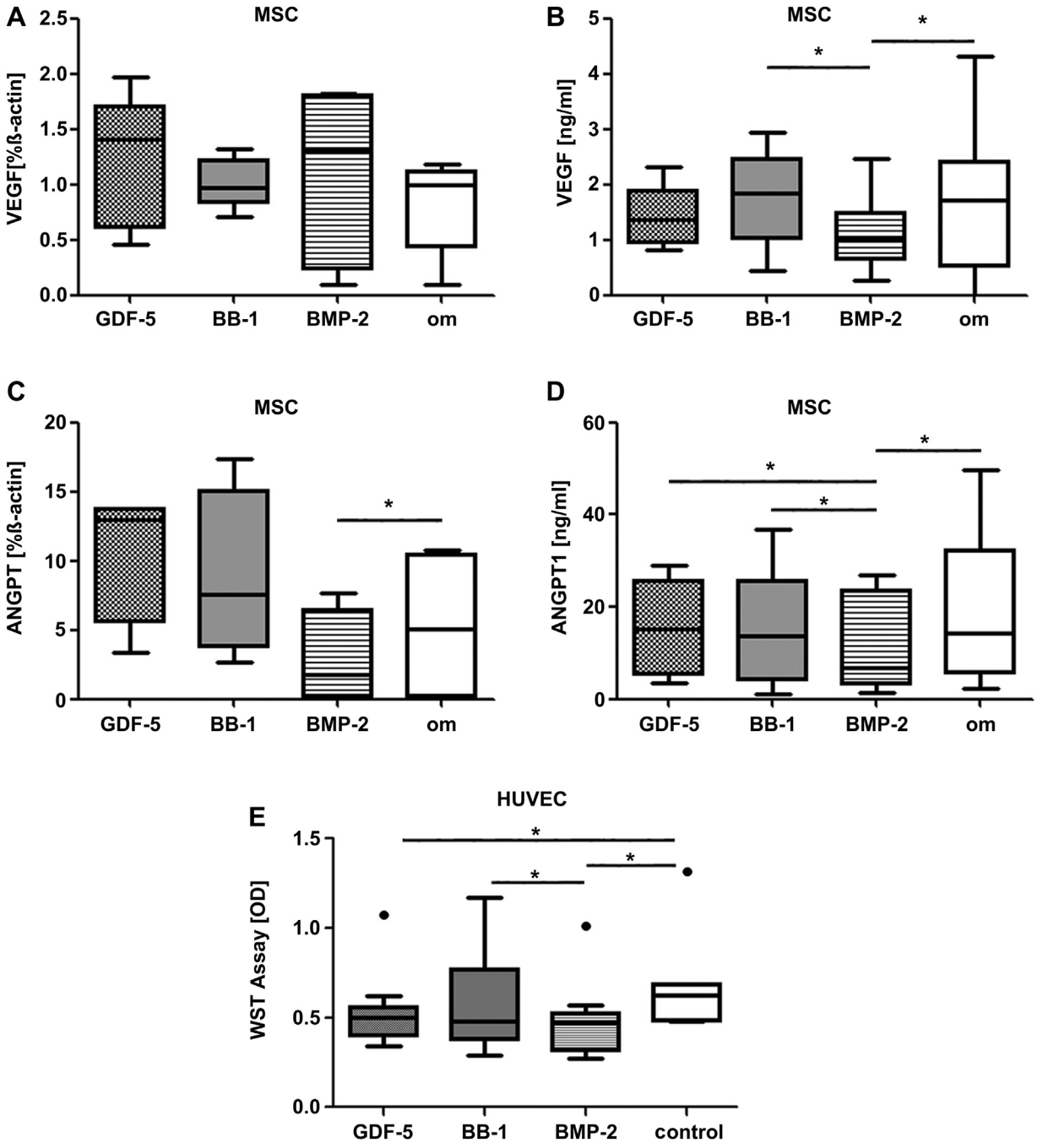

Fig. 2. Effects of growth factors on angiogenic parameters. MSC were cultured in osteogenic medium (om) in monolayer and 500 ng/ml GDF-5, BB-1, BMP-2 or no growth factor were added. After 21 days of culture VEGF mRNA levels (A) and ANGPT1 gene expression levels (C) were quantified by qPCR and normalized to the housekeeping gene β-actin. B, D) Culture supernatants were collected from all MSC groups (6 donors) at day 12 and 21 after a 3 day incubation period and duplicate samples were tested for VEGF (B) and ANGPT1 protein (D) by ELISA. Data are from 6 experiments, with duplicate cultures from 6 donors. E) HUVEC cultures were incubated with BMP-2, BB-1 or GDF-5 for 24 h before metabolic activity was evaluated by a WST assay in duplicates. Data are from 3 experiments with cells from 4 donors. Boxplots reflect the 25th and 75th percentile as boxes, the median as horizontal line and minimum and maximum values as whiskers. Data points presented as dots in graph E mark matched outliers following Tukey's algorithm for depiction purposes. Asterisks mark statistical differences between groups with p-values <0.05 regarded as significant.

3.6. BB-1 promoted corticalis and bone marrow cavity formation

Already 4 weeks post surgery the callus had a decentralized micromorphology with a starting cavity formation in 78% (7/9) of BB-1 treated animals, an effect seen in only 1/9 GDF-5 and in none of the BMP-2 treated defects at this time point (Table 2). After 8 weeks, in all of the BB-1 treated defects the radius endings were reconnected with hollow bone containing a continuous medullar cavity, transitioned into bone marrow cavities of the radius endings. In contrast, none of the BMP-2 and only 1/9 of the GDF-5 treated defects showed a morphology similar to BB-1 - not even at 12 weeks. At the 12 week time point 56% of BMP-2 treated defects were filled with spongy callus over the total defect length. In contrast, 89% (8/9) of the GDF-5 treated animals showed decentralized bone with a cortical structure and medullar cavity formation over at least 25–75% of the defect region (Table 2).

Author's personal copy

Table 2
Overview of defect bridging, pseudo joint-formation and bone marrow cavity formation in rabbit critical size defects.

Weeks	Defect bridging			Joint formation			Cavity formed (25–75% defect)			Cavity formed (>75% defect)			Cavity reconnected (100% defect)
	4	8	12	4	8	12	4	8	12	4	8	12	12
Control	0/7	0/7	0/7	0/7	0/7	0/7	0/7	0/7	0/7	0/7	0/7	0/7	0/7
BMP-2	3/9	9/9	9/9	7/9	0/9	0/9	0/9	0/9	4/9	0/9	0/9	0/9	0/9
GDF-5	5/9	8/9	8/9	7/9	5/9	5/9	1/9	8/9	8/9	0/9	1/9	4/9	1/9
BB-1	9/9	9/9	9/9	1/9	0/9	0/9	7/9	9/9	9/9	0/9	9/9	9/9	9/9

In the middle of the defects microarchitecture of the callus was variable between animals of the same group according to transverse micro-CT reconstruction (Fig. 5A, Supplementary Fig. S1 G–I, Supplementary Videos 1–4). However, while no larger marrow cavity was evident in BMP-2 treated defects, marrow cavity was reconstituted in all BB-1 treated rabbits. In GDF-5 treated defects half of the defects reformed cavities (Supplementary Fig. S1 G–I, Supplementary Videos 1–4). Histological examination of trichrome stained sections ($n = 2$/group/direction of cutting) of BB-1 treated defects showed bone marrow with hematopoietic tissue islands and adipose cells surrounded by vascular sinuses interspersed within a meshwork of trabecular bone. In contrast, BMP-2 callus appeared massive with only small leakage areas at the previous proximal and distal defect endings. Thus, GDF-5 and its variant BB-1 attracted more hematopoietic tissue than BMP-2 during bone regeneration and showed a better hollow bone reconstruction than BMP-2.

3.7. Vascularization of bone in growth factor induced callus

Endothelial structures were stained 12 weeks post surgery using an anti-CD31 antibody (Fig. 5D). Longitudinal and transverse slices from the compact region of newly built bone ($n = 2$ animals/group/direction of cutting) revealed a tighter vascularization in GDF-5 and BB-1 treated defects than in BMP-2 treated and untreated defects. Findings were not quantified by histomorphometry or stereology due to the low number of replicates.

3.8. Micromorphology and bone mineral density are comparable to healthy bone with BB-1

When micromorphology of defects was compared to the contralateral healthy long bone (Fig. 6), only BB-1 effected a microarchitecture comparable to that of healthy radius in all analyzed parameters. The mean trabecular number (Tb.N) was 19.4-fold lower in calluses of BB-1 treated animals than in saline treated control defects ($p < 0.001$), 13.2-fold lower than in BMP-2 and 12.1-fold lower than in GDF-5 treated defects ($p < 0.001$). Confirmatively, the mean trabecular thickness (Tb.Th) was lower in BB-1 induced defects and in healthy bone than in BMP-2, GDF-5 and control defects ($p < 0.001$), while the mean trabecular separation (Tb.Sp) was wider, accordingly ($p < 0.001$). Density of the medullar bone region was 5-fold lower in BB-1 callus and in healthy bone than in BMP-2 treated and in saline treated defects ($p < 0.001$). BMP-2 callus consisted predominantly of woven bone with micro morphological parameters that differed only slightly from spontaneous bone formation in control defects.

Table 3
Primers used for gene expression analysis.

Gene	Primer
ALP	5′-CAC CAC GAG AGT GAA CCA TG-3′
	5′-CAA TTC TGC CTC CTT CCA CC-3′
ANGPT1	5′-GGT TGG ACT GTA ATA CAA CAT-3′
	5′-TTC CCT TCC CAG TCC ATT AA-3′
ANGPT2	5′-GCT ATG TGC TTA AAA TAC ACC TT-3′
	5′-GGC TGT CCC TGT AAG TCC TT-3′
VEGF	5′-TGA GTT AAA CGA ACG TAC TTG-3′
	5′-GTC GAT GGT GAT GGT GTG G-3′
β-Actin	5′-TGA CGG GGT CAC CCA CAC TG-3′
	5′-CTA GAA GCA TTT GCG GTG GAC G-3′

4. Discussion

Among the classical BMP types developed for therapeutic stimulation of new bone formation, GDF-5 attracted less interest, since it was originally isolated from cartilage [31], was regarded as a the major stabilizer of cartilage during joint formation [32–34] and induced less bone in rodents compared to BMP-2 [35]. Surprisingly little information is, thus, available on the capacity of GDF-5 for healing of critical size defects in long bones [20].

In line with a disparate osteogenic activity and biological function, GDF-5 and BMP-2 show a distinct interaction with the BMP type I and II receptors, an activity regarded as crucial for the great variety of biological functions between members of the TGF-β superfamily. While the BMP-2 molecule binds to BMPR-IA and BMPR-IB with little discrimination of both subtypes, GDF-5 has a lower binding activity to BMPR-IA than BMPR-IB [36]. Based on rational drug design, we recently swapped two amino acids in the BMPR-I binding sequence of GDF-5 to residues present in the BMP-2 molecule [22]. We now demonstrated that this new GDF-5 mutant BB-1 displays an about 10-fold increased binding affinity to BMPR-IA at unaltered BMPR-IB and BMPR-II affinity, meaning it acquired an activity like BMP-2 to bind BMPR-I with little discrimination of both subtypes. As intended, BB-1 enhanced ALP activation of C2C12 cells expressing predominantly BMPR-IA, and increased the ALP activity in human MSC undergoing osteogenesis compared to GDF-5, producing values like BMP-2. Thus, by generating BB-1, we succeeded to create a mutant GDF-5 molecule with enhanced osteogenesis, confirming that a biological activity seen for BMP-2 on rodent and human progenitor cells was transferred to the mutant protein.

Since only two amino acids in GDF-5 were exchanged to obtain BB-1, we considered it unlikely that angiogenic properties ascribed to GDF-5 would be destroyed in the new molecule, except they depended on a disparate activation of BMPR-IA and BMPR-IB. Although we expected, according to studies in rodents [21,37,38], that GDF-5 and BB-1 treatment may stimulate human MSC to enhanced expression of the angiogenic molecules VEGF and ANGPT1, we rather observed no such effect for GDF-5 and BB-1 compared to controls, but noticed some suppressive activity for BMP-2. We here studied a range of concentrations of the growth factors in our *in vitro* analysis looking on 14.8–1200 ng/ml in rodent C2C12 cells and on 5, 50 and 500 ng/ml for testing of human cells. By this we wanted adhere to published literature and exclude overlooking important differences that may occur when effects of some growth factors plateau, while the others continue to increase like this was seen on C2C12.

Author's personal copy

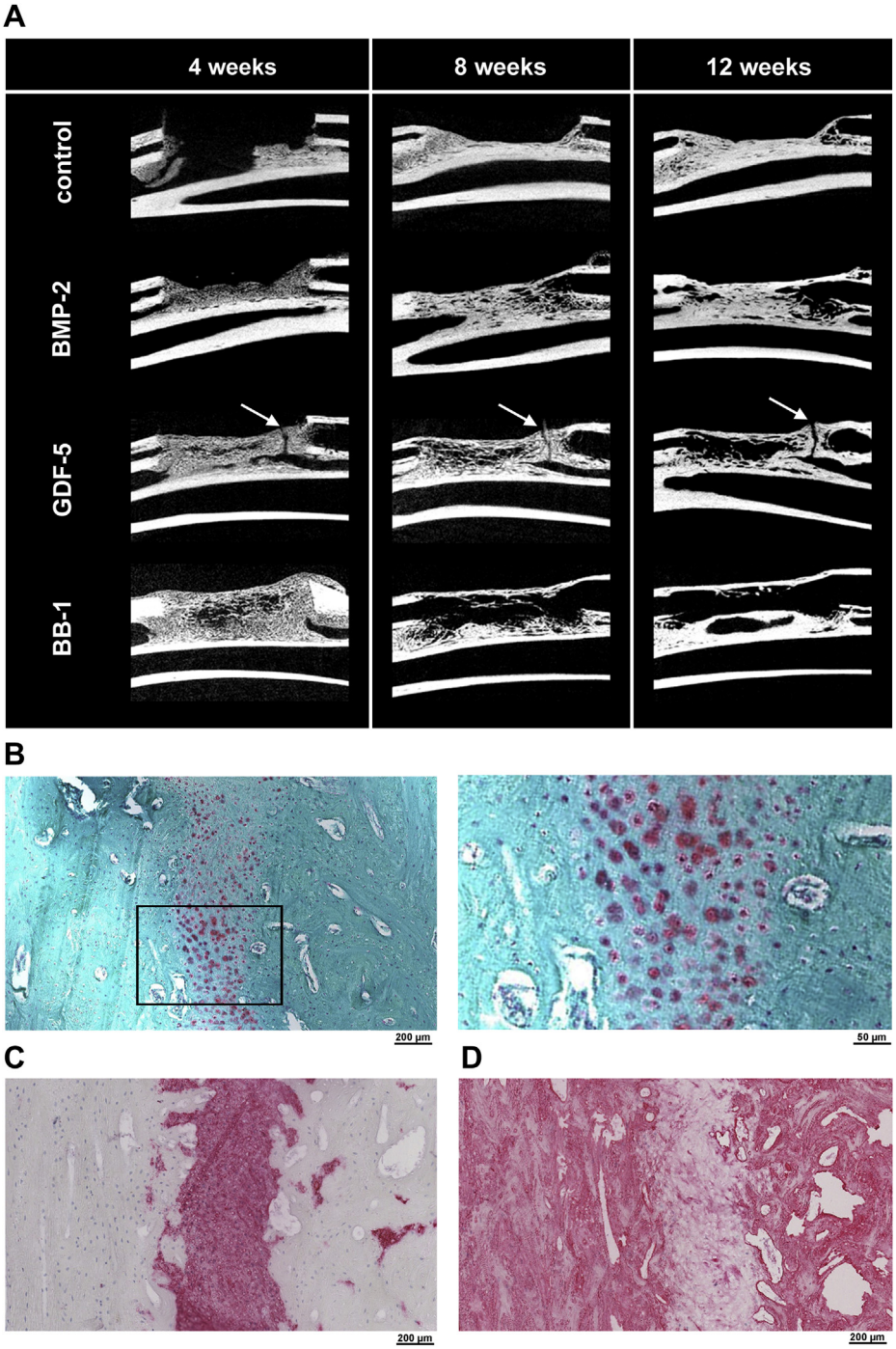

Fig. 3. Effects of growth factors on bone bridging. A) Representative longitudinal slices of reconstructed Micro-CT scans of the 15 mm critical size defect region in rabbit radiuses. Follow-up *in vivo* micro-CT scans show reconstructed longitudinal cuts of one and the same animal as representative for each treatment group at 4, 8 and 12 weeks post surgery. Joint-like gap formation is marked by arrows. B–D) Gap-region in longitudinal slices of a critical size defect treated with 50 µg wild-type GDF-5 after 12 weeks. Staining for glycosaminoglycans (Safranin-O-Fast-green, B), for collagen-type-II (C) and for collagen-type-I (D). Scale bars = 200 µm.

According to histology of two animals per group, the denser vascularization observed in central defect regions in GDF-5 and BB-1 treated animals compared to BMP-2 and control defects is a first indication for similar and superior angiogenic properties of GDF-5 and BB-1 as opposed to BMP-2 which is in line with previous work [37]. We currently address quantitative aspects of these promising pilot data in a separate follow-up study based on µCT and histology choosing earlier time points in the same animal model than in the current study.

VEGF and ANGPT1 secretion by bone marrow derived human MSC undergoing *in vitro* osteogenesis is interesting in view of a recently reported arrest of bone formation by BMP-2 in the endosteal cavity in mice [39]. Minear et al. ascribed this site-specific effect of BMP-2 to β-catenin dependent Wnt signaling on osteoblast differentiation of distinct progenitor cell populations (marrow-derived as opposed to periosteum derived). Our *in vitro* data on human MSC suggest that BMP-2 may reduce some angiogenic features of bone marrow derived progenitor cells compared

Author's personal copy

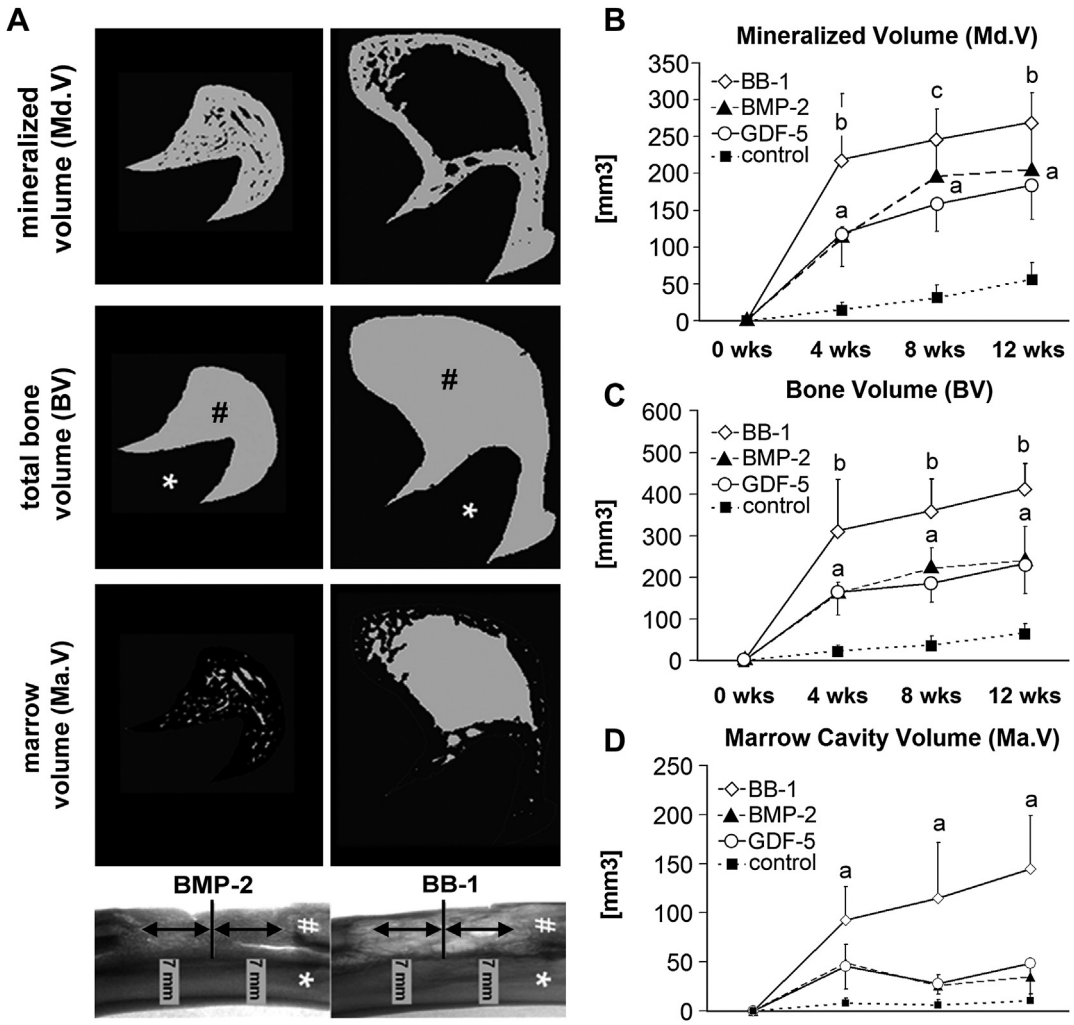

Fig. 4. Quantification of neobone formation by *in vivo* follow-up micro CT scans over 12 weeks. A) Representative micro-CT images in the mid-plane of a BB-1 and BMP-2 treated defect to depict the methodology of structural parameter analysis: Mineralized Volume (Md.V, B) determines radiopaque tissue inside the defect region excluding all cavities; Bone Volume (BV, C) determines the total volume of callus including all pores and cavities, and Marrow cavity Volume (Ma.V, D) represents cavities implemented by radiopaque callus as defined by ASBMR nomenclature. The ulna is marked by * and the newly formed callus by #. The region of interest included the defect over 14 mm, extending 7 mm proximal and 7 mm distal from the mid-plane excluding the ulna (bottom). Data from $n = 7$ rabbits per group are presented as mean ± SD (* vs controls, ≠ vs GDF-5 and controls, # vs all).

to GDF-5 or BB-1. It would next be interesting to compare the underlying molecular pathways and mechanisms of osteogenesis and angiogenesis between BMP-2 and BB-1 now that a comparable interaction with BMP-signaling receptors could be shown.

The advantage of the critical size defect model chosen in this study is that no instrumentation is required to stabilize the defect since radius and ulna of rabbits are fused at the bone endings. This confers a higher reproducibility of results between animals. We further achieved that a quantitative follow-up of neobone formation was possible within the same animal by *in vivo* micro-CT analysis which was so far only possible for rats [40]. To allow high resolution scans of anesthetised rabbits we newly constructed an *in vivo* micro-CT system for rabbit legs. The chosen 18 μm resolution required about 20–25 min of scanning time per time point and we cannot rule out that this repeated radiation exposure did not affect bone regeneration. Since, however, all groups obtained exactly the same radiation dose this should not have introduced a bias regarding differences between groups. A general advantage of choosing the rabbit was that the size of the long bone defect (15 mm) can better approach a clinical situation allowing better imitation of distance-relevant factors like cell attraction, angiogenesis and remodeling. Most importantly however, opposite to rodents, the cortical bone of higher order animals contains the haversian system [41] which is deemed to be important for cortical bone healing. Furthermore, the efficacy of growth factors like BMP-2 is known to reduce with higher order animals and long bone healing in rodents is characterized by double cortical callus formation [42,43]; a phenomenon not observed in other species. The decision not to choose other larger animal models like the dog [44] was based on ethical considerations.

The most surprising finding of this study was that BMP-2 affected quality and micromorphology of the bony callus differently from GDF-5 and especially BB-1: While BMP-2 callus was dense and spongy, the callus showed a more decentralized micromorphology in GDF-5 treated animals. Remarkably, this difference between BMP-2 and GDF-5 treated defects was not due to a distinct mineralized callus size at 4 weeks or thereafter (Fig. 4) in accordance with earlier findings in alveolar ridges in dogs [8]. Although histology from early time points is not available, we suggest, in line with the chondroproliferative capacity of

Author's personal copy

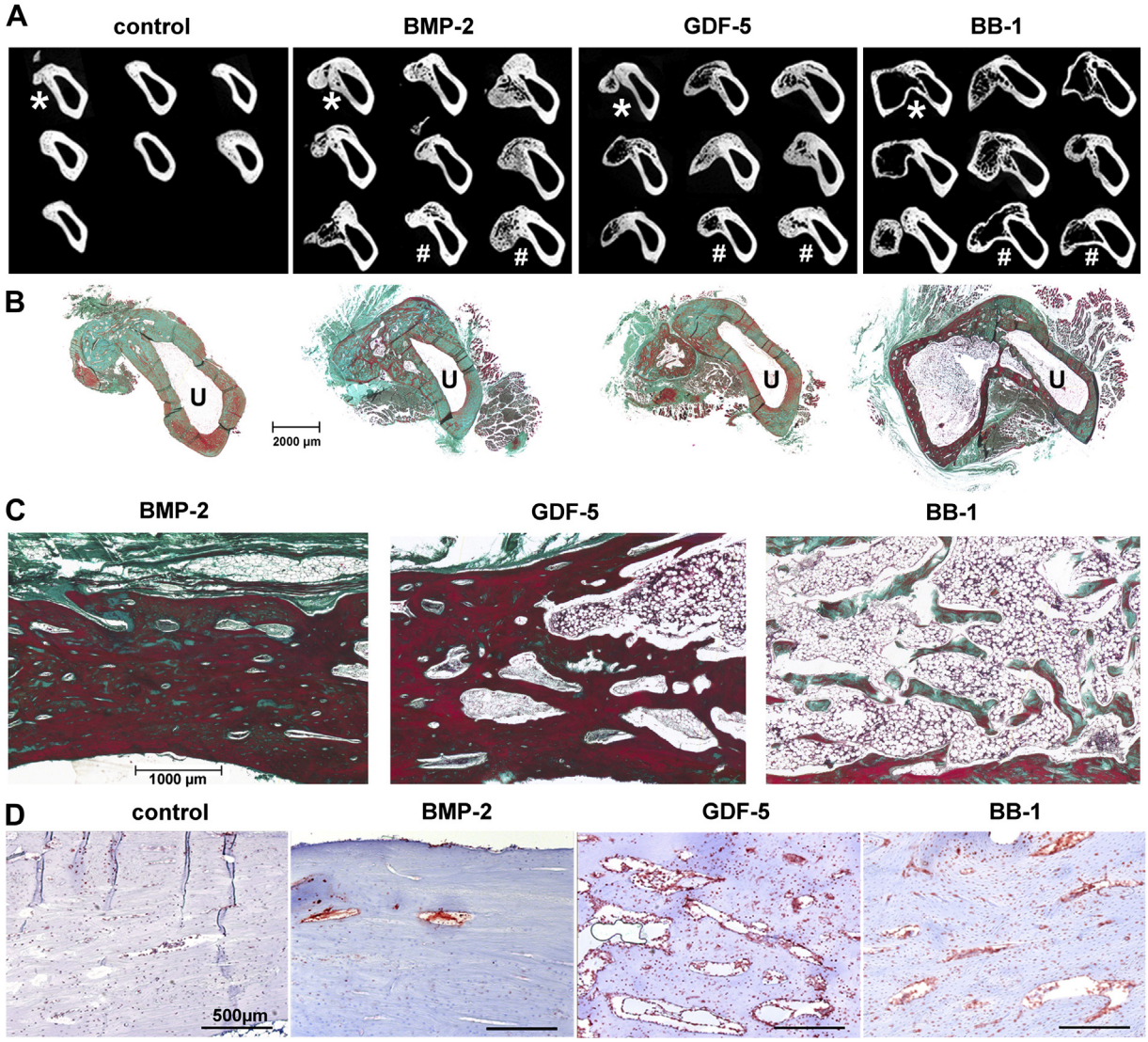

Fig. 5. Corticalis, marrow cavity formation and vascularization of bone regenerates. Rabbit radius critical size defects were treated with collagen sponges containing 20 µg (main study) or 50 µg (marked by #) of recombinant GDF-5, BB-1 or BMP-2 proteins, respectively. Controls were handled analogously refraining from protein. A) Overview of transverse images in the defect middle of reconstructed micro-CT scans of all animals 12 weeks post surgery. B) Masson–Goldner Trichrome staining of transverse slices from the defect middle. The corresponding micro-CT images are depicted in A) by asterisk. The ulna is marked by U. C) Longitudinal slices stained by Masson–Goldner. Extensive bone marrow was rebuilt in newly formed cavernous calluses of BB-1 treated rabbits. D) Endothelial staining with anti-CD31-antibody of longitudinal slices from the middle of defects.

GDF-5 [33], that more cartilage is formed in the GDF-5 treated defects. When this cartilage undergoes hypertrophy, an enhanced matrix remodeling activity, attraction of more blood vessels and thus a distinct endochondral bone formation pattern [45] may result. Obviously, triggering the osteochondral route of bone formation could favor corticalis and bone marrow cavity formation and thus the bona fide structure created via endochondral bone formation during development. Inherent to GDF-5 was, however, a cartilage stabilizing activity at sites of enhanced mechanical stress conferring cartilaginous pseudojoint persistence in 5/9 GDF-5 treated animals up to 12 weeks after surgery. Cartilage morphogenesis is a multistep cascade that includes factors for initiation, promotion, and maintenance of the cartilage phenotype [46]. In contrast, BMP-2 may rather stimulate the direct route of osteoblast formation from osteoprogenitors, resulting in a differing angiogenesis and matrix remodeling and denser woven bone like in desmal bone formation. A predominance of dense woven bone was previously also seen for BMP-2 in other studies [6,12], and reported for OP-1 in a dog model [44]. BMP-2 may, thus not be the only BMP-type with such an activity.

A recent study in rats compared GDF-5 and BMP-2 regarding regeneration of critical size defects in long bones [20]. Defects were treated with 50 µg growth factor per 5 mm defect, even a higher dose than used here (20 µg in a 15 mm defect) in rabbits. In the rat, GDF-5 induced less callus and delayed tissue mineralization but a higher rate of bone per total callus volume compared to BMP-2. This is only partly consistent with the data of our control groups underlining the discussed disparity between rodent and higher order animal models. Decisively, by combining positive features of GDF-5 and BMP-2, the newly designed mutant BB-1 not only increased callus volume and earlier bridging, but resulted in fast remodeling of a hollow long bone with a reconnected bone marrow cavity in all treated animals without a complication of persisting cartilage tissue.

Author's personal copy

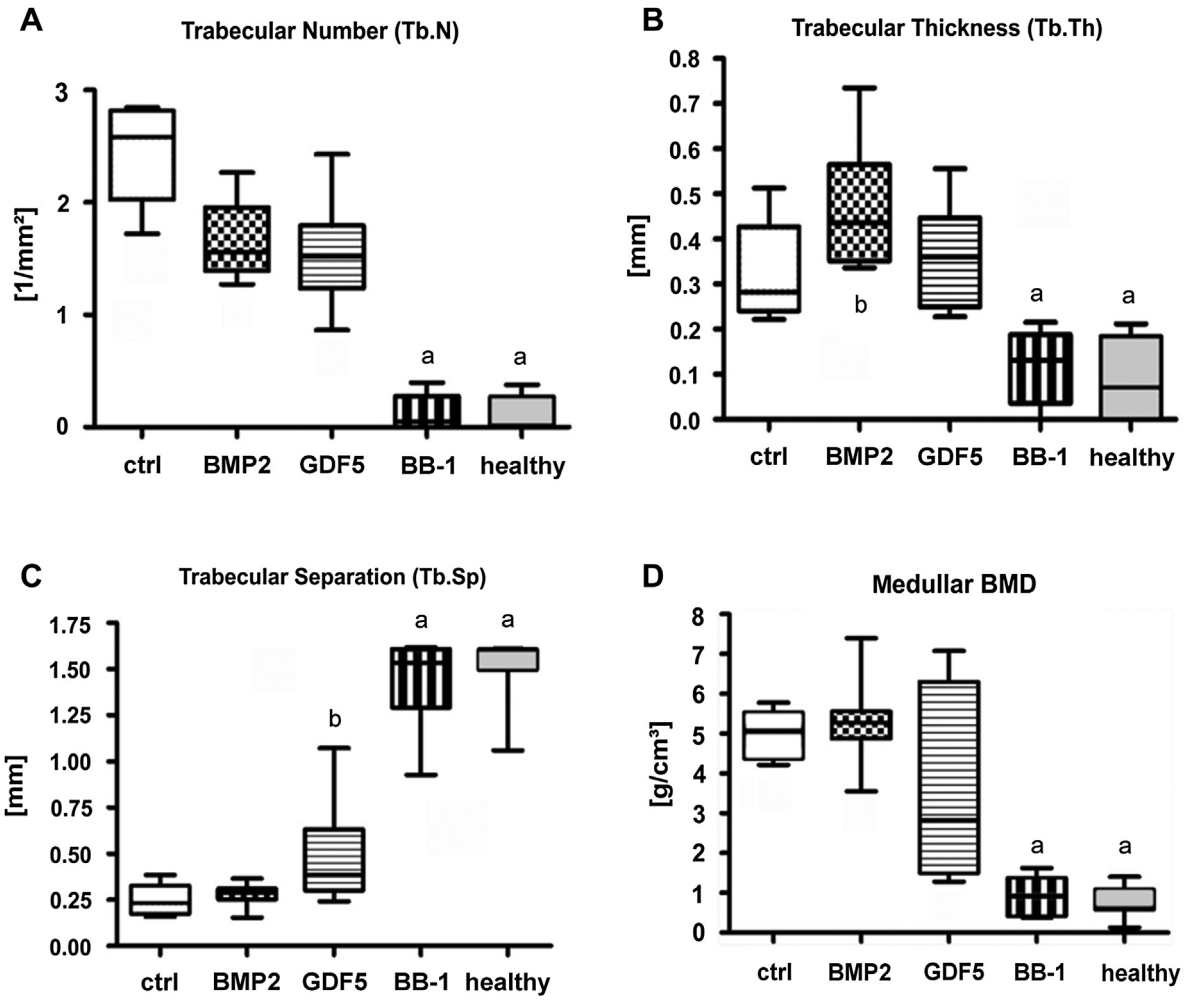

Fig. 6. Microarchitecture and medullar bone mineral density of regenerated bone tissue. Callus micromorphology was determined by micro-CT 12 weeks post surgery in comparison to contralateral healthy bone. (# vs all, * vs ctrl, BMP-2 and GDF-5, ≠ vs ctrl) Note the high variability of the micro structure of the medullar region for GDF-5 treated animals. Boxplots depict the 25th and 75th percentile as boxes, the median as horizontal line and minimum and maximum values as whiskers from $n = 7$ rabbits per group.

5. Conclusion

Altogether our study thus demonstrated that we created with BB-1 an attractive new GDF-5 variant with enhanced osteogenicity and long bone formation capacity combining not only positive features of GDF-5 and BMP-2 but avoiding also negative aspects of these same molecules. Most importantly, given the here observed differences between BMP-2 and BB-1 will persist in patients, our data for the first time recommend to consider a site specific application of distinct members of the BMP family of growth factors for bone healing. While the mainly spongy neo-bone formation capacity of BMP-2 could be more favorable for desmal bone defects like in the skull, GDF-5 based factors like BB-1 are attractive for regeneration of large long bone defects. Here quick restoration of corticalis and marrow-cavity is desired without an unwanted side effect of persistent pseudojoint formation. BB-1 could, thus, become highly valuable as a therapeutic agent for long bone treatment.

Sponsor

Contract grant sponsor: Stiftung Orthopaedische Universitaetsklinik Heidelberg.

Acknowledgments

The authors thank Phil Salmon and Markus Heneka for their advice and support in designing and application of the “Hasitom” in vivo-micro-CT device, Eric Steck, Joerg Fellenberg and Heiner Saehr for technical advice, Jeannine Holschbach and Kathrin Brohm for assistance in animal experiments and Simone Ganz for assistance with statistical analysis.

Appendix A. Supplementary data

Supplementary data related to this article can be found at http://dx.doi.org/10.1016/j.biomaterials.2013.04.029.

References

[1] Glowacki J. Angiogenesis in fracture repair. Clin Orthop Relat Res 1998:S82–9.
[2] Grellier M, Granja PL, Fricain JC, Bidarra SJ, Renard M, Bareille R, et al. The effect of the co-immobilization of human osteoprogenitors and endothelial cells within alginate microspheres on mineralization in a bone defect. Biomaterials 2009;30:3271–8.
[3] Weiss S, Zimmermann G, Pufe T, Varoga D, Henle P. The systemic angiogenic response during bone healing. Arch Orthop Trauma Surg 2009;129:989–97.
[4] Geiger F, Bertram H, Berger I, Lorenz H, Wall O, Eckhardt C, et al. Vascular endothelial growth factor gene-activated matrix (VEGF165-GAM) enhances

Author's personal copy

osteogenesis and angiogenesis in large segmental bone defects. J Bone Miner Res 2005;20:2028–35.
[5] Schipani E, Maes C, Carmeliet G, Semenza GL. Regulation of osteogenesis-angiogenesis coupling by HIFs and VEGF. J Bone Miner Res 2009;24:1347–53.
[6] Bax BE, Wozney JM, Ashhurst DE. Bone morphogenetic protein-2 increases the rate of callus formation after fracture of the rabbit tibia. Calcif Tissue Int 1999;65:83–9.
[7] Bostrom M, Lane JM, Tomin E, Browne M, Berberian W, Turek T, et al. Use of bone morphogenetic protein-2 in the rabbit ulnar nonunion model. Clin Orthop Relat Res 1996:272–82.
[8] Schwarz F, Rothamel D, Herten M, Ferrari D, Sager M, Becker J. Lateral ridge augmentation using particulated or block bone substitutes biocoated with rhGDF-5 and rhBMP-2: an immunohistochemical study in dogs. Clin Oral Implants Res 2008;19:642–52.
[9] Niikura T, Hak DJ, Reddi AH. Global gene profiling reveals a downregulation of BMP gene expression in experimental atrophic nonunions compared to standard healing fractures. J Orthop Res 2006;24:1463–71.
[10] Alt V, Donell ST, Chhabra A, Bentley A, Eicher A, Schnettler R. A health economic analysis of the use of rhBMP-2 in Gustilo-Anderson grade III open tibial fractures for the UK, Germany, and France. Injury 2009;40:1269–75.
[11] Katagiri T, Takahashi N. Regulatory mechanisms of osteoblast and osteoclast differentiation. Oral Dis 2002;8:147–59.
[12] Bouxsein ML, Turek TJ, Blake CA, D'Augusta D, Li X, Stevens M, et al. Recombinant human bone morphogenetic protein-2 accelerates healing in a rabbit ulnar osteotomy model. J Bone Joint Surg Am 2001;83-A:1219–30.
[13] Jung RE, Thoma DS, Hammerle CH. Assessment of the potential of growth factors for localized alveolar ridge augmentation: a systematic review. J Clin Periodontol 2008;35:255–81.
[14] Francis-West PH, Abdelfattah A, Chen P, Allen C, Parish J, Ladher R, et al. Mechanisms of GDF-5 action during skeletal development. Development 1999;126:1305–15.
[15] Chhabra A, Zijerdi D, Zhang J, Kline A, Balian G, Hurwitz S. BMP-14 deficiency inhibits long bone fracture healing: a biochemical, histologic, and radiographic assessment. J Orthop Trauma 2005;19:629–34.
[16] Magit DP, Maak T, Trioano N, Raphael B, Hamouria Q, Polzhofer G, et al. Healos/recombinant human growth and differentiation factor-5 induces posterolateral lumbar fusion in a New Zealand white rabbit model. Spine (Phila Pa 1976) 2006;31:2180–8.
[17] Simank HG, Herold F, Schneider M, Maedler U, Ries R, Sergi C. Growth and differentiation factor 5 (GDF-5) composite improves the healing of necrosis of the femoral head in a sheep model. Analysis of an animal model. Orthopade 2004;33:68–75.
[18] Yoshimoto T, Yamamoto M, Kadomatsu H, Sakoda K, Yonamine Y, Izumi Y. Recombinant human growth/differentiation factor-5 (rhGDF-5) induced bone formation in murine calvariae. J Periodontal Res 2006;41:140–7.
[19] Depprich R, Handschel J, Sebald W, Kubler NR, Wurzler KK. Comparison of the osteogenic activity of bone morphogenetic protein (BMP) mutants. Mund Kiefer Gesichtschir 2005;9:363–8.
[20] Wulsten D, Glatt V, Ellinghaus A, Schmidt-Bleek K, Petersen A, Schell H, et al. Time kinetics of bone defect healing in response to BMP-2 and GDF-5 characterised by in vivo biomechanics. Eur Cell Mater 2011;21:177–92.
[21] Kadomatsu H, Matsuyama T, Yoshimoto T, Negishi Y, Sekiya H, Yamamoto M, et al. Injectable growth/differentiation factor-5-recombinant human collagen composite induces endochondral ossification via Sry-related HMG box 9 (Sox9) expression and angiogenesis in murine calvariae. J Periodont Res 2008;43:483–9.
[22] Kasten P, Beyen I, Bormann D, Luginbuhl R, Ploger F, Richter W. The effect of two point mutations in GDF-5 on ectopic bone formation in a beta-tricalciumphosphate scaffold. Biomaterials 2010;31:3878–84.
[23] Heinecke K, Seher A, Schmitz W, Mueller TD, Sebald W, Nickel J. Receptor oligomerization and beyond: a case study in bone morphogenetic proteins. BMC Biol 2009;7:59.
[24] Dexheimer V, Mueller S, Braatz F, Richter W. Reduced reactivation from dormancy but maintained lineage choice of human mesenchymal stem cells with donor age. PLoSOne 2011;6:e22980.
[25] Dickhut A, Dexheimer V, Martin K, Lauinger R, Heisel C, Richter W. Chondrogenesis of human mesenchymal stem cells by local transforming growth factor-beta delivery in a biphasic resorbable carrier. Tissue Eng Part A 2010;16:453–64.
[26] Janicki P, Boeuf S, Steck E, Egermann M, Kasten P, Richter W. Prediction of in vivo bone forming potency of bone marrow-derived human mesenchymal stem cells. Eur Cell Mater 2011;21:488–507.
[27] Stanford CM, Jacobson PA, Eanes ED, Lembke LA, Midura RJ. Rapidly forming apatitic mineral in an osteoblastic cell line (UMR 106-01 BSP). J Biol Chem 1995;270:9420–8.
[28] Baudin B, Bruneel A, Bosselut N, Vaubourdolle M. A protocol for isolation and culture of human umbilical vein endothelial cells. Nat Protoc 2007;2:481–5.
[29] Parfitt AM, Drezner MK, Glorieux FH, Kanis JA, Malluche H, Meunier PJ, et al. Bone histomorphometry: standardization of nomenclature, symbols, and units. Report of the ASBMR Histomorphometry Nomenclature Committee. J Bone Miner Res 1987;2:595–610.
[30] Sebald W, Nickel J, Zhang JL, Mueller TD. Molecular recognition in bone morphogenetic protein (BMP)/receptor interaction. Biol Chem 2004;385:697–710.
[31] Chang SC, Hoang B, Thomas JT, Vukicevic S, Luyten FP, Ryba NJ, et al. Cartilage-derived morphogenetic proteins. New members of the transforming growth factor-beta superfamily predominantly expressed in long bones during human embryonic development. J Biol Chem 1994;269:28227–34.
[32] Erlacher L, McCartney J, Piek E, ten DP, Yanagishita M, Oppermann H, et al. Cartilage-derived morphogenetic proteins and osteogenic protein-1 differentially regulate osteogenesis. J Bone Miner Res 1998;13:383–92.
[33] Buxton P, Edwards C, Archer CW, Francis-West P. Growth/differentiation factor-5 (GDF-5) and skeletal development. J Bone Joint Surg Am 2001;83-A(Suppl. 1):S23–30.
[34] Seemann P, Schwappacher R, Kjaer KW, Krakow D, Lehmann K, Dawson K, et al. Activating and deactivating mutations in the receptor interaction site of GDF5 cause symphalangism or brachydactyly type A2. J Clin Invest 2005;115:2373–81.
[35] Yoshimoto T, Yamamoto M, Kadomatsu H, Sakoda K, Yonamine Y, Izumi Y. Recombinant human growth/differentiation factor-5 (rhGDF-5) induced bone formation in murine calvariae. J Periodontal Res 2006;41(2):140–7.
[36] Nickel J, Kotzsch A, Sebald W, Mueller TD. A single residue of GDF-5 defines binding specificity to BMP receptor IB. J Mol Biol 2005;349:933–47.
[37] Yamashita H, Shimizu A, Kato M, Nishitoh H, Ichijo H, Hanyu A, et al. Growth/differentiation factor-5 induces angiogenesis in vivo. Exp Cell Res 1997;235:218–26.
[38] Zeng Q, Li X, Beck G, Balian G, Shen FH. Growth and differentiation factor-5 (GDF-5) stimulates osteogenic differentiation and increases vascular endothelial growth factor (VEGF) levels in fat-derived stromal cells in vitro. Bone 2007;40:374–81.
[39] Minear S, Leucht P, Miller S, Helms JA. rBMP represses Wnt signaling and influences skeletal progenitor cell fate specification during bone repair. J Bone Miner Res 2010;25:1196–207.
[40] Gasser JA, Ingold P, Grosios K, Laib A, Hammerle S, Koller B. Noninvasive monitoring of changes in structural cancellous bone parameters with a novel prototype micro-CT. J Bone Miner Metab 2005;(23 Suppl.):90–6.
[41] Nunamaker DM. Experimental models of fracture repair. Clin Orthop Relat Res 1998;(355 Suppl.):S56–65.
[42] Gerstenfeld LC, Alkhiary YM, Krall EA, Nicholls FH, Stapleton SN, Fitch JL, et al. Three-dimensional reconstruction of fracture callus morphogenesis. J Histochem Cytochem 2006;54:1215–28.
[43] Isaksson H, Grongroft I, Wilson W, van Donkelaar CC, van RB, Tami A, et al. Remodeling of fracture callus in mice is consistent with mechanical loading and bone remodeling theory. J Orthop Res 2009;27:664–72.
[44] Salkeld SL, Patron LP, Barrack RL, Cook SD. The effect of osteogenic protein-1 on the healing of segmental bone defects treated with autograft or allograft bone. J Bone Joint Surg Am 2001;83-A:803–16.
[45] Oliveira SM, Mijares DQ, Turner G, Amaral IF, Barbosa MA, Teixeira CC. Engineering endochondral bone: in vivo studies. Tissue Eng Part A 2009;15:635–43.
[46] Reddi AH. Cartilage morphogenetic proteins: role in joint development, homoeostasis, and regeneration. Ann Rheum Dis 2003;62(Suppl. 2):ii73–8.